Progress In Electromagnetics Research, PIER 87, 1–14, 2008

TIME DOMAIN INTEGRAL EQUATION APPROACH FOR ANALYSIS OF TRANSIENT RESPONSES BY METALLIC-DIELECTRIC COMPOSITE BODIES

G. H. Zhang and M. Y. Xia

School of Electronics Engineering and Computer Science
Peking University
Beijing 100871, China

C. H. Chan

Department of Electronic Engineering
City University of Hong Kong
Hong Kong SAR, China

Abstract—A time domain integral equation approach for analysis of transient responses by 3D composite metallic-dielectric bodies is proposed, which is formulated using the surface equivalent polarization and magnetization as unknown functions. The time domain electric field integral equation is adopted for the metallic part, while the time domain Piggio-Miller-Chang-Harrington-Wu integral equations are adopted for the dielectric part. The spatial and temporal basis functions are the Rao-Wilton-Glisson functions and quadratic B-spline functions, respectively. Numerical examples are provided to demonstrate the stability and accuracy of the proposed method. No late-time instability is encountered, and the results are found in good agreements with analytical or moment method solutions.

1. INTRODUCTION

Time domain simulation methods have received increasing attention in recent years due to the needs for transient analyses in many emerging short-impulse and broadband applications, such as ultra-wideband antennas and communication systems, short-impulse responses of targets, high-speed digital circuits and transient phenomenon in nonlinear components. Finite difference time domain (FDTD) method has been the dominant tool for time domain simulations; however,

time domain integral equation (TDIE) approach is preferable in some aspects especially for analysis of transient scattering by large-size bodies, because it solves fewer unknowns using surface discretization and unnecessitates the artificial absorbing boundary condition (ABC). One reason that prevents TDIE approach from general acceptance is the lack of a definitive stability condition, in contrast to the Courant stability condition in FDTD methods. To suppress the late-time instability in TDIE methods, many measures have been attempted, including the averaging or filtering techniques [1–4], using different formulations [5], the improved temporal basis functions [6–10], and accurate evaluations of matrix elements [11, 12]. By intuition, we believe that the late-time instability is nonphysical unlike the grid dispersion in FDTD, so that it should not be present as long as (i) the rigorousness of the governing equations, (ii) the completeness of the temporal basis functions, and (iii) the accuracy of the matrix elements are assured. Keeping this in mind, we derived a set of TDIE formulations with equivalent polarizations and magnetizations as unknown functions by (i) enforcing the rigorous boundary conditions, (ii) using the complete quadratic B-spline temporal basis functions, and (iii) calculating the matrix elements to sufficient precision. Indeed, in our previous works on wire structures, 3D conducting and dielectric bodies [13–15], no late-time instability has been encountered and all numerical results are accurate compared with those obtained by frequency domain method of moments (MoM). The purpose of this work is to extend the methodology to transient scattering by 3D metallic-dielectric composite bodies.

Analyses of scattering by 3D metallic-dielectric composite bodies have wide applications, such as the typical platform-antenna-radome structures. At a single frequency point or for a narrow frequency range, the MoM is undoubtfully the first choice. For broadband or transient scattering analysis, the time domain MoM, i.e., the TDIE methods should be the preferred approach. A TDIE procedure using the time domain electric field integral equations (TD-EFIE) has been reported in [16, 17]. However, in this paper, we will use the time domain Poggio-Miller-Chang-Harrington-Wu (TD-PMCHW) equations that were found harder to stabilize than the TD-EFIE or the time domain magnetic field integral equation (TD-MFIE) for dielectric bodies [18]. The use of the combined-field type TD-PMCHW equations is important in terms of eliminating the possible spurious solutions near the resonant frequencies, because either TD-EFIE or TD-MFIE for conducting bodies has been found to give wrong results near these frequency points when the data in time domain are transformed to frequency domain [19, 20].

The organization of the paper is as follows. Section 2 is dedicated to formulations by employing the induced equivalent polarization and magnetization as unknown functions. In the past, induced equivalent electric and magnetic currents are commonly used as unknown functions, by which extra temporal integrals have to be performed to find the electric and magnetic charges to calculate the scalar potentials [6, 16, 19]. To avoid doing the integrals, the governing equations, i.e., the boundary conditions, are differentiated with respect to time [7, 9, 10, 14]. This would, however, weaken the equations as they implicitly permit time slow-varying solutions which might incur the low-frequency breakdown known as the exponential divergence. The present formulations are devoid of these two disadvantages. Section 3 shows numerical validations using a coated sphere, a semi-metallic and semi-dielectric sphere, and a composite missile model as examples, followed by some concluding remarks at the end in Section 4.

2. FORMULATION

Refer to Figure 1. The metallic surface is denoted by S_1, the dielectric surface denoted by S_2, and the metallic-dielectric contacted surface denoted by S_3. A transient wave is incident upon the composite body, which induce a distribution of equivalent polarization $\mathbf{P}_{1s}$ on S_1, distributions of polarization $\mathbf{P}_{2s}$ and magnetization $\mathbf{M}_{2s}$ on S_2, and a distribution of polarization $\mathbf{P}_{3s}$ on S_3. The equivalent electric and magnetic currents and charges on each surface can be found through $\mathbf{P}_s$ and $\mathbf{M}_s$, i.e., $\mathbf{J}_s = \partial\mathbf{P}_s/\partial t$, $\sigma_s = -\nabla_s \cdot \mathbf{P}_s$, $\mathbf{J}_{ms} = \partial(\mu_0\mathbf{M}_s)/\partial t$ and $\sigma_{ms} = -\nabla_s \cdot (\mu_0\mathbf{M}_s)$. The continuity equations are satisfied automatically. The equivalent polarization and magnetization in the present work amounts to the 'new source vectors' introduced in [21].

In the open region V_0, the scattered fields can be expressed by

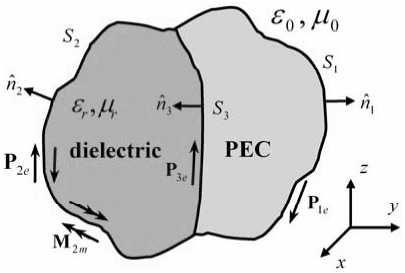

Figure 1. Geometry of transient scattering by a 3D composite body.

$\mathbf{P}_{1s}$, $\mathbf{P}_{2s}$ and $\mathbf{M}_{2s}$ as

$$\mathbf{E}^s = -\eta_0 \left[\mathbf{L}_1\left(\mathbf{P}_{1s}\right) + \mathbf{L}_2\left(\mathbf{P}_{2s}\right)\right] + \mathbf{K}_2\left(\tilde{\mathbf{M}}_{2s}\right), \quad \mathbf{r} \in V_0 \tag{1a}$$

$$\mathbf{H}^s = -[\mathbf{K}_1(\mathbf{P}_{1s}) + \mathbf{K}_2(\mathbf{P}_{2s})] - \frac{1}{\eta_0}\mathbf{L}_2(\tilde{\mathbf{M}}_{2s}), \quad \mathbf{r} \in V_0 \tag{1b}$$

where $\eta_0 = \sqrt{\mu_0/\varepsilon_0}$ is the intrinsic impedance of the free-space, $\tilde{\mathbf{M}}_{2s} = \mu_0 \mathbf{M}_{2s}$, and the two operators are defined by

$$\mathbf{L}_q(\mathbf{X}) = \frac{c}{4\pi}\int_{S_q}\left[\frac{\partial^2 \mathbf{X}\left(\mathbf{r}', t - R/c\right)}{R\partial(ct)^2} - \nabla\frac{\left[\nabla' \cdot \mathbf{X}\left(\mathbf{r}', t'\right)\right]_{t'=t-R/c}}{R}\right] dS', \quad q = 1, 2 \tag{2a}$$

$$\mathbf{K}_q(\mathbf{X}) = -\frac{c}{4\pi}\nabla \times \int_{S_q} \frac{\partial \mathbf{X}\left(\mathbf{r}', t - R/c\right)}{R\partial(ct)} dS', \quad q = 1, 2 \tag{2b}$$

in which $c = 1/\sqrt{\mu_0\varepsilon_0}$ is the light velocity in vacuum. In the dielectric region V_d, the transmitted field can be expressed by $-\mathbf{P}_{2s}$, $-\mathbf{M}_{2s}$ and $\mathbf{P}_{3s}$ as

$$\mathbf{E}^d = -\eta_d \left[\mathbf{L}_2^d\left(-\mathbf{P}_{2s}\right) + \mathbf{L}_3^d\left(\mathbf{P}_{3s}\right)\right] + \mathbf{K}_2^d\left(-\tilde{\mathbf{M}}_{2s}\right), \ \mathbf{r} \in V_d \tag{3a}$$

$$\mathbf{H}^d = -\left[\mathbf{K}_2^d\left(-\mathbf{P}_{2s}\right) + \mathbf{K}_3^d\left(\mathbf{P}_{3s}\right)\right] - \frac{1}{\eta_d}\mathbf{L}_2^d\left(-\tilde{\mathbf{M}}_{2s}\right), \ \mathbf{r} \in V_d \tag{3b}$$

where $\eta_d = \eta_r\eta_0$ with $\eta_r = \sqrt{\mu_r/\varepsilon_r}$, while $\mathbf{L}_q^d$ and $\mathbf{K}_q^d$ are the same as (2a)–(2b) by replacing c with $c_d = c/\sqrt{\mu_r\varepsilon_r}$.

By enforcing the electric tangential components to vanish on S_1 and S_3, i.e., $\hat{n}_1 \times (\mathbf{E}^i + \mathbf{E}^s) = 0$ and $\hat{n}_3 \times \mathbf{E}^d = 0$, we have

$$\hat{n}_1 \times \eta_0 \left[\mathbf{L}_1(\mathbf{P}_{1s}) + \mathbf{L}_2\left(\mathbf{P}_{2s}\right)\right] - \hat{n}_1 \times \mathbf{K}_2\left(\tilde{\mathbf{M}}_{2s}\right) = \hat{n}_1 \times \mathbf{E}^i, \ \mathbf{r} \in S_1 \tag{4a}$$

$$\hat{n}_3 \times \eta_d \left[\mathbf{L}_2^d\left(\mathbf{P}_{2s}\right) - \mathbf{L}_3^d\left(\mathbf{P}_{3s}\right)\right] - \hat{n}_3 \times \mathbf{K}_2^d\left(\tilde{\mathbf{M}}_{2s}\right) = 0, \ \mathbf{r} \in S_3 \tag{4b}$$

Applying the electric and magnetic tangential continuity conditions on S_2, i.e., $\hat{n}_2 \times (\mathbf{E}^i + \mathbf{E}^s) = \hat{n}_2 \times \mathbf{E}^d$ and $\hat{n}_2 \times (\mathbf{H}^i + \mathbf{H}^s) = \hat{n}_2 \times \mathbf{H}^d$, we obtain the TD-PMCHW equations:

$$\begin{aligned}\hat{n}_2 \times \Big[&\eta_0 \mathbf{L}_1\left(\mathbf{P}_{1s}\right) + \left(\eta_0\mathbf{L}_2 + \eta_d\mathbf{L}_2^d\right)\left(\mathbf{P}_{2s}\right) - \eta_d\mathbf{L}_3^d\left(\mathbf{P}_{3s}\right) \\ &- \left(\tilde{\mathbf{K}}_2 + \tilde{\mathbf{K}}_2^d\right)\left(\tilde{\mathbf{M}}_{2s}\right)\Big] = \hat{n}_2 \times \mathbf{E}^i, \quad \mathbf{r} \in S_2\end{aligned} \tag{5a}$$

$$\begin{aligned}\hat{n}_2 \times \Big[&\tilde{\mathbf{K}}_1\left(\mathbf{P}_{1s}\right) + \left(\tilde{\mathbf{K}}_2 + \tilde{\mathbf{K}}_2^d\right)\left(\mathbf{P}_{2s}\right) - \tilde{\mathbf{K}}_3^d\left(\mathbf{P}_{3s}\right) \\ &+ \left(\frac{1}{\eta_0}\mathbf{L}_2 + \frac{1}{\eta_d}\mathbf{L}_2^d\right)\left(\tilde{\mathbf{M}}_{2s}\right)\Big] = \hat{n}_2 \times \mathbf{H}^i, \quad \mathbf{r} \in S_2\end{aligned} \tag{5b}$$

Eqns. (4a)–(5b) are the governing equations to be solved for the unknown equivalent sources.

Expand $\mathbf{P}_{qs}(\mathbf{r}', t')$ $(q = 1, 2, 3)$ and $\tilde{\mathbf{M}}_{2s}(\mathbf{r}', t')$ by employing the RWG spatial basis functions [22] and the quadratic B-spline temporal basis functions [13]:

$$\mathbf{P}_{qs}\left(\mathbf{r}', t'\right) = \sum_{j=1}^{\infty} \sum_{n=1}^{N_q} c_{qn}(j) S\left(\bar{t}' - j\right) \mathbf{f}_{qn}\left(\mathbf{r}'\right), \ q = 1, 2, 3 \quad \text{(6a)}$$

$$\tilde{\mathbf{M}}_{2s}\left(\mathbf{r}', t'\right) = \eta_d \sum_{j=1}^{\infty} \sum_{n=1}^{N_q} d_{2n}(j) S\left(\bar{t}' - j\right) \mathbf{f}_{2n}\left(\mathbf{r}'\right) \quad \text{(6b)}$$

where $\mathbf{f}_{qn}(\mathbf{r}')$ $(n = 1, 2, \ldots, N_q)$ are the RWG basis functions defined on S_q. The total number of edges of the triangulated S_1 is N_1, including the joint edges, where a joint edge connects a pair of triangles with one triangle on S_1 and the other on S_2. The total number of edges of the triangulated S_3 is N_3, including the joint edges, where a joint edge connects a pair of triangles with one triangle on S_3 and the other on S_2. The total number of edges of the triangulated S_2 is N_2, excluding any joint edge that connects a triangle on S_1 or S_3. The η_d on the right-hand side of (6b) allows $d_{2n}(j)$ to be on the same order of magnitude as $c_{2n}(j)$. The temporal basis function $S(\bar{t}')$ is taken to be the quadratic B-spline functions:

$$S\left(\bar{t}'\right) = \begin{cases} \frac{1}{2}\left(\bar{t}' + 1\right)^2, & 0 \le \bar{t}' + 1 < 1 \\ \frac{1}{2} + \bar{t}' - \bar{t}'^2, & 0 \le \bar{t}' < 1 \\ \frac{1}{2} - \left(\bar{t}' - 1\right) + \frac{1}{2}\left(\bar{t}' - 1\right)^2, & 0 \le \bar{t}' - 1 < 1. \end{cases} \quad (7)$$

where $\bar{t}' = t'/\Delta t$ with Δt the time-step size. Because $S'(\bar{t}')$ is continuous and $S(\bar{t}') = S'(\bar{t}') = 0$ at the ends ($\bar{t}' = -1$ and $\bar{t}' = 2$), the transitions of the expanded current and charge are 'naturally' smooth at the temporal nodes, which permits point-matching.

Substituting (6a)–(6b) into (4a)–(5b), and then testing them with $\hat{n}_p \times \mathbf{f}_{pm}(\mathbf{r})\delta(\bar{t} - i)$ $(p = 1, 2, 3;\ m = 1, 2, \ldots, N_p;\ i = 1, 2, \ldots)$, we obtain their discrete forms:

$$\sum_{j=1}^{\infty} \begin{pmatrix} \left[L_{11}(i-j)\right]\left\{c_1(j)\right\} + \left[L_{12}(i-j)\right]\left\{c_2(j)\right\} \\ -\eta_r \left[K_{12}(i-j)\right]\left\{d_2(j)\right\} \end{pmatrix} = \left\{\tilde{E}_1(i)\right\} \quad \text{(8a)}$$

$$\sum_{j=1}^{\infty} \begin{pmatrix} \left[L_{32}^d(i-j)\right]\left\{c_2(j)\right\} - \left[L_{33}^d(i-j)\right]\left\{c_3(j)\right\} \\ -\left[K_{32}^d(i-j)\right]\left\{d_2(j)\right\} \end{pmatrix} = \{0\} \quad \text{(8b)}$$

$$\sum_{j=1}^{\infty}\begin{pmatrix}[L_{21}(i-j)]\{c_1(j)\}+[L_{22}(i-j)\\ +\eta_r L_{22}^d(i-j)]\{c_2(j)\}-\eta_r\left[L_{23}^d(i-j)\right]\{c_3(j)\}\\ -\eta_r\left[K_{22}(i-j)+K_{22}^d(i-j)\right]\{d_2(j)\}\end{pmatrix}=\left\{\tilde{E}_2(i)\right\} \quad (9a)$$

$$\sum_{j=1}^{\infty}\begin{pmatrix}[K_{21}(i-j)]\{c_1(j)\}+[K_{22}(i-j)\\ +K_{22}^d(i-j)]\{c_2(j)\}-\left[K_{23}^d(i-j)\right]\{c_3(j)\}\\ +\left[\eta_r L_{22}(i-j)+L_{22}^d(i-j)\right]\{d_2(j)\}\end{pmatrix}=\{H_2(i)\} \quad (9b)$$

where $[L_{pq}(j)]$ and $[K_{pq}(j)]$ are $(N_p\times N_q)$ interacting matrices for field points on S_p and source locations on S_q; $\{c_q(j)\}$ is a $N_q\times 1$ unknown column vector while $\{\tilde{E}_p(i)\}$ is a $N_p\times 1$ excitation column vector; and so forth. The elements are calculated by

$$[L_{pq}(j)]_{mn}=\int_{T_{pm}}\mathbf{f}_{pm}(\mathbf{r})\cdot\mathbf{L}_q\left(\mathbf{f}_{qn}\left(\mathbf{r}'\right)S\left(j-\bar{R}\right)\right)dS,\ p,q=1,2,3 \quad (10a)$$

$$[K_{pq}(j)]_{mn}=\int_{T_{pm}}\mathbf{f}_{pm}(\mathbf{r})\cdot\mathbf{K}_q\left(\mathbf{f}_{qn}\left(\mathbf{r}'\right)S\left(j-\bar{R}\right)\right)dS,\ p,q=1,2,3 \quad (10b)$$

$$\left\{\tilde{E}_p(i)\right\}_m=\frac{1}{\eta_0}\int_{T_{pm}}\mathbf{f}_{pm}(\mathbf{r})\cdot\mathbf{E}^i(\mathbf{r},i\Delta t)dS,\quad p=1,2 \quad (11a)$$

$$\{H_2(i)\}_m=\int_{T_{2m}}\mathbf{f}_{2m}(\mathbf{r})\cdot\mathbf{H}^i(\mathbf{r},i\Delta t)dS \quad (11b)$$

where $\bar{R}=R/(c\Delta t)$ and T_{pm} denotes a pair of triangles connected by the mth edge on the surface S_p. Due to the compactness of the temporal basis functions, we have $-1<j-\bar{R}<2$ or $\bar{R}_{\min}-1<j<\bar{R}_{\max}+2$, where $R_{\min}=0$ and $R_{\max}$ is the dimension of the whole composite body; therefore, $0\le j\le D_0=\mathrm{int}(\bar{R}_{\max}+2)$, where $\mathrm{int}(\cdot)$ means taking the integer part. That is, we have $[L_{pq}(j)]=[K_{pq}(j)]=[0]$ if $j<0$ or $j>D_0$. The calculation of $[L_{pq}^d(j)]$ and $[K_{pq}^d(j)]$ are the same as (10a)–(10b) by replacing $\mathbf{L}_q$ and $\mathbf{K}_q$ with $\mathbf{L}_q^d$ and $\mathbf{K}_q^d$, and replacing $\bar{R}$ with $\bar{R}^d=R/(c_d\Delta t)$. Similarly, we have $[L_{pq}^d(j)]=[K_{pq}^d(j)]=[0]$ if $j<0$ or $j>D_d$ with $D_d=\mathrm{int}[R_{\max}^d/(c_d\Delta t)+2]$, where $R_{\max}^d$ is the dimension of the dielectric part.

Combining (8a)–(9b) and making the index exchange $j\leftrightarrow i-j$, we obtain the final equation in the marching-on-in-time (MOT) form

$$[A(0)]\{x(i)\}=\{b(i)\}-\sum_{j=1}^{\min(i-1,D)}[A(j)]\{x(i-j)\} \quad (12)$$

where $D = \max(D_0, D_d)$, the system matrix, unknown vector and excitation vector are

$$[A] = \begin{bmatrix} L_{11} & L_{12} & -\eta_r K_{12} & 0 \\ L_{21} & L_{22}+\eta_r L_{22}^d & -\eta_r(K_{22}+K_{22}^d) & -\eta_r L_{23}^d \\ K_{21} & K_{22}+K_{22}^d & \eta_r L_{22}+L_{22}^d & -K_{23}^d \\ 0 & L_{32}^d & -K_{32}^d & -L_{33}^d \end{bmatrix} \tag{13a}$$

$$\{x\} = \begin{pmatrix} c_1 \\ c_2 \\ d_2 \\ c_3 \end{pmatrix}, \quad \{b\} = \begin{pmatrix} \tilde{E}_1 \\ \tilde{E}_2 \\ H_2 \\ 0 \end{pmatrix} \tag{13b}$$

Once (12) is solved for $\{c_1(j)\}_{j=1}^{N_t}$, $\{c_2(j)\}_{j=1}^{N_t}$, $\{d_2(j)\}_{j=1}^{N_t}$ and $\{c_3(j)\}_{j=1}^{N_t}$, where N_t is the time sequential length of the equivalent sources that have been resolved, the transient scattering far-field may be found via (1a) by

$$\mathbf{E}^s_{\text{far}-\text{zone}}(\mathbf{r},t) =$$

$$\hat{r}\times\hat{r}\times\frac{c}{4\pi}\sum_{q=1}^{2}\int_{S_q}\frac{\partial^2}{\partial(ct)^2}\left[\eta_0\mathbf{P}_{qs}\left(\mathbf{r}',t-R/c\right)-\hat{r}\times\tilde{\mathbf{M}}_{qs}\left(\mathbf{r}',t-R/c\right)\right]\frac{dS'}{R}\approx$$

$$-\frac{1}{r}\frac{1}{(c\Delta t)^2}\frac{c}{4\pi}\sum_{q=1}^{2}\sum_{j=1}^{N_t}\sum_{n=1}^{N_q}\left\{\hat{\theta}\left[\eta_0 c_{qn}(j)\hat{\theta}+\eta_d d_{qn}(j)\hat{\phi}\right]\right.$$

$$\left.+\hat{\phi}\left[\eta_0 c_{qn}(j)\hat{\phi}-\eta_d d_{qn}(j)\hat{\theta}\right]\right\}\cdot\mathbf{F}_{qn}\left(\bar{\tau}-j\right) \tag{14a}$$

$$\mathbf{F}_{qn}\left(\bar{\tau}\right)=\int_{T_{qn}}\mathbf{f}_{qn}\left(\mathbf{r}'\right)S"(\bar{\tau}+\hat{r}\cdot\bar{\mathbf{r}}')dS', \quad q=1,2 \tag{14b}$$

where $\bar{\tau}=\bar{t}-\bar{r}$ is the far-field time-step, $\bar{r}=r/(c\Delta t)$, $\bar{\mathbf{r}}'=\mathbf{r}'/(c\Delta t)$, and $\hat{r}=\hat{x}\sin\theta\cos\phi+\hat{y}\sin\theta\sin\phi+\hat{z}\cos\theta$ with (θ,ϕ) being the scattering direction in spherical coordinate system. Taking the Fourier transform of (14a), i.e., carrying out the Fourier transform of (14b), we can find the scattered far-field in frequency domain and calculate the radar cross-section (RCS) for a range of frequency.

3. NUMERICAL RESULTS

In this section, three examples are provided to demonstrate the stability and accuracy of the TDIE approach described above. The

incident wave is assumed to be the modulated Gaussian pulse given by

$$\mathbf{E}^i(\mathbf{r},t) = \hat{u}E_0 \exp\left[-\left(\frac{\tau - t_0}{\sqrt{2}\sigma}\right)^2\right]\cos(2\pi f_0 \tau) \tag{15}$$

where $E_0 = 120\pi$, f_0 is the centre carrier frequency, $t_0 = 8\sigma$ and $\sigma = 6/(2\pi f_{bw})$ with f_{bw} being the nominal bandwidth, $\hat{u} = \hat{x}$ denotes the polarized state, $\tau = t - \mathbf{r}\cdot\hat{k}/c$ with $\hat{k} = -\hat{z}$ indicating the incident direction.

First, to compare with the analytical MIE series solutions, we consider a conducting sphere of diameter 0.4 m coated by a dielectric shell with thickness 0.05 m and relative permittivity $\varepsilon_r = 2.0$, which is modeled with 4,404 unknowns using the RWG basis functions. In this example, $f_0 = 500\,\text{MHz}$, $f_{bw} = 1.0\,\text{GHz}$, $\Delta t = 0.125\,\text{ns}$ or $c\Delta t = 0.0375\,\text{LM}$ (LM=light meter: the time that light takes to travel 1 m in vacuum) are used. The evolution of induced electric currents and induced magnetic currents at the point (0, 0, 0.25 m) are displayed in Figures 2(a) and Figure 2(b) till 10 LM (the program is actually terminated at 2,000 time-steps or 75 LM without instability, which levels off about 10^{-15}). The wideband mono-static RCS from zero frequency to 1.0 GHz is obtained and compared in good agreements with the analytical MIE series solutions as shown in Figure 2(c).

The second example is a mixture model composed by a conducting hemisphere and a dielectric hemisphere with $\varepsilon_d = 2\varepsilon_0$. The diameter of the composite sphere is 0.5 m, and the total number of unknowns is 5,171. We again use $f_0 = 500\,\text{MHz}$ and $f_{bw} = 1.0\,\text{GHz}$, but $\Delta t = 0.1\,\text{ns}$ or $c\Delta t = 0.03\,\text{LM}$. The evolutions of induced electric currents at the point (0, 0, -0.25 m) and magnetic currents at the point (0, 0, 0.25 m) are pictured in Figures 3(a) and 3(b) (the program is terminated at 2,000 time-steps or 60 LM without instability). The wideband mono-static RCS from zero frequency to 1.0 GHz is computed as shown in Figure 3(c). To check the accuracy, RCS data at a set of discrete frequency points are obtained by using the MoM in frequency domain, which are found in good agreements with the TDIE results. For the TDIE and MoM, the surface meshing and quadrature rule are identical.

For the last example, we consider a suppositional missile model, which is composed of an elliptical dielectric head with $\varepsilon_d = 2\varepsilon_0$ and a PEC trunk, with the coordinate origin at the center of the bottom surface. The whole length of this composite body is 5.5 m, and the total number of unknowns is 3,350. The incident wave is incident against the head of the target, and $f_0 = 100\,\text{MHz}$, $f_{bw} = 200\,\text{MHz}$, and $\Delta t = 0.5\,\text{ns}$ ($c\Delta t = 0.15\,\text{LM}$) have been used. The evolution of induced magnetic currents at the point (5.06, 0.07, 0.07 m) is displayed in

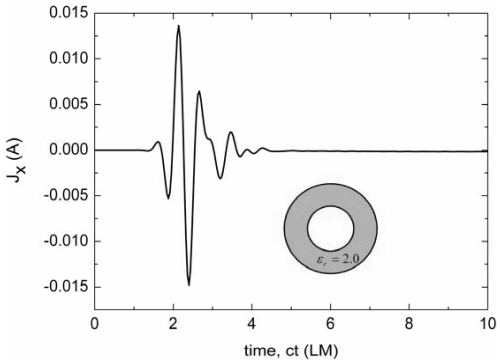

(a)

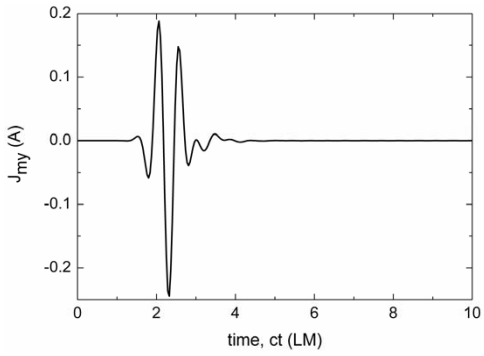

(b)

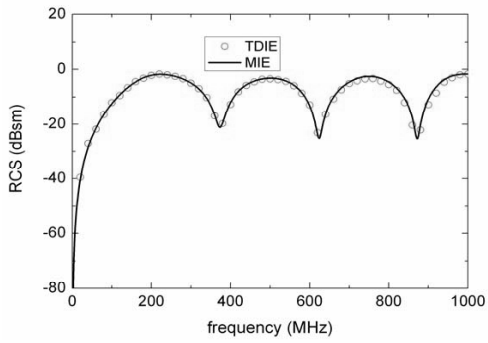

(c)

Figure 2. Responses of a coated sphere to a modulated Gaussian impulse. (a) The induced electric current at the point (0, 0, 0.25 m), (b) induced magnetic current at the point (0, 0, 0.25 m), and (c) wideband mono-static RCS from 0 to 1 GHz and comparison with analytical solution.

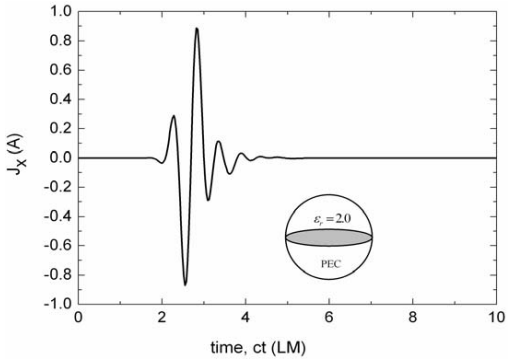

(a)

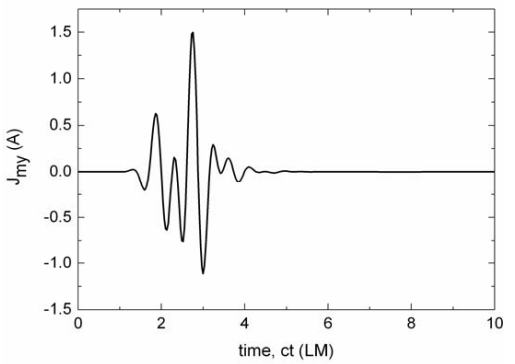

(b)

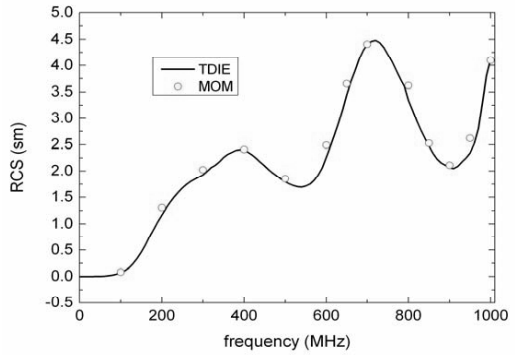

(c)

Figure 3. Responses of a composite sphere to a modulated Gaussian impulse. (a) The induced electric current at the point $(0, 0, -0.25\,\mathrm{m})$, (b) induced magnetic current at the point $(0, 0, 0.25\,\mathrm{m})$, and (c) wideband mono-static RCS from 0 to 1 GHz and comparison with MoM solution.

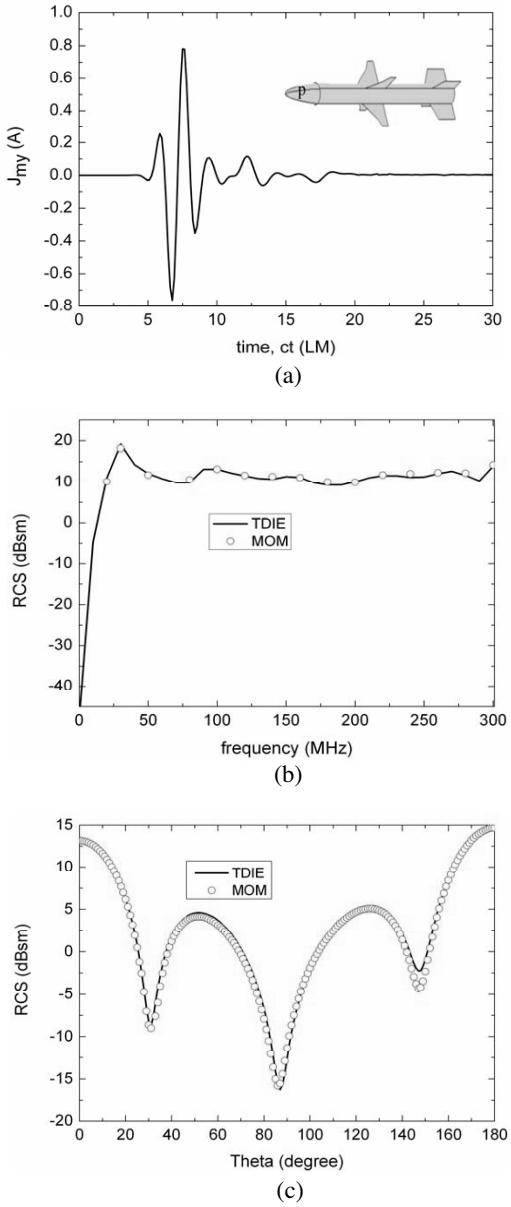

Figure 4. Responses of a model missile to a modulated Gaussian impulse. (a) The induced electric current at the point P, (b) wideband mono-static RCS from 0 to 300 MHz and comparison with MoM solution, and (c) bi-static RCS in the E-plane at 100 MHz and comparison with MoM solution.

Figure 4(a) (the program is terminated at 180 LM without instability). The wideband mono-static RCS from zero frequency to 300 MHz is displayed in Figure 4(b). The E-plane bi-static RCS at 100 MHz is obtained and found in reasonable agreements with the MoM solutions as shown in Figure 4(c).

4. CONCLUDING REMARKS

A time domain integral equation (TDIE) approach for analysis of transient scattering problems by 3D metallic and dielectric composite objects is presented, which is formulated by using the equivalent polarization and magnetization as unknown sources. The time domain electric field integral equation is used for the metallic part, while the time domain Piggio-Miller-Chang-Harrington-Wu integral equations are used for the dielectric part. The governing equations are derived by directly enforcing the genuine boundary conditions rather than their differential forms, and no derivative is replaced by difference. The Rao-Wilton-Glisson functions and quadratic B-spline functions are employed as the spatial and temporal basis functions, respectively. Evaluations of matrix elements are carried out analytically for self-actions and numerically to high precision for inter-actions. Though rigorous stability condition is still elusive, numerical examples demonstrate that the proposed TDIE scheme is stable, because no low-frequency exponential divergence or high-frequency oscillating divergence is observed. The results are found in good agreements with analytical or moment method solutions.

ACKNOWLEDGMENT

This work is supported by the NSFC Project 60771001 and 60825102. Computing platform is provided by the Center for Computational Science & Engineering (CCSE) of Peking University.

REFERENCES

1. Rynne, B. P. and P. D. Smith, "Stability of time-marching algorithms for electric field integral equation," *Journal of Electromagnetic Waves and Applications*, Vol. 4, 1181–1205, 1990.
2. Rynne, B. P., "Time domain Scattering from arbitrary surfaces using the electric field integral equation," *Journal of Electromagnetic Waves and Applications*, Vol. 5, 93–112, 1991.

3. Davies, P. J., "Stability of time-marching numerical schemes for the electric field integral equation," *Journal of Electromagnetic Waves and Applications*, Vol. 8, 85–114, 1994.
4. Davies, P. J. and D. B. Duncan, "Averaging techniques for time-marching schemes for retarded potential integral equations," *App. Numer. Math.*, Vol. 23, 291–310, 1997.
5. Lesha, M. J. and F. J. Paoloni, "Transient scattering from arbitrary conducting surfaces by iterative solution of the electric field integral equation," *Journal of Electromagnetic Waves and Applications*, Vol. 10, 1139–1167, 1996.
6. Manara, G., A. Monorchio, and R. Reggiannini, "A space-time discretization criterion for a stable time-marching solution of the electric field integral equation," *IEEE T. Antenn. Propag.*, Vol. 45, 527–532, 1997.
7. Hu, J. L. and C. H. Chan, "Improved temporal basis functions using for time domain electric field integral equation method," *Electro. Lett.*, Vol. 35, 883–885, 1999.
8. Chung, Y. S., T. K. Sarker, B. H. Jung, et al., "Solution of a time domain magnetic-field integral equation for arbitrarily closed conducting bodies using an unconditionally stable methodology," *Microw. Opt. Technol. Lett.*, Vol. 35, 493–499, 2002.
9. Weile, D. S., G. Pisharody, N. W. Chen, B. Shanker, and E. Michielssen, "A novel scheme for the solution of the time-domain integral equations of electromagnetics," *IEEE T. Antenn. Propag.*, Vol. 52, 283–295, 2004.
10. Jiang, G. X., H. B. Zhu, G. Q. Ji, and W. Cao, "Improved stable scheme for the time domain integral equation method," *IEEE Microw. Wirel. Compon. Lett.*, Vol. 17, 1–3, 2007.
11. Bluck, M. J. and S. P. Walker, "Time-domain BIE analysis of large three-dimensional electromagnetic scattering problems," *IEEE T. Antenn. Propag.*, Vol. 45, 894–901, 1997.
12. Lu, M. and E. Michielssen, "Closed form evaluation of time domain fields due to Rao-Wilton-Glisson sources for use in marching-on-in-time based EFIE solvers," *IEEE APS. Int. Symp. Dig.*, 74–77, 2002.
13. Xia, M. Y., G. H. Zhang, G. L. Dai, et al., "Stable solution of time domain integral equation methods using quadratic B-spline temporal basis functions," *J. Comput. Math.*, Vol. 25, 374–384, 2007.
14. Wang, P., M. Y. Xia, J. M. Jin, and L. Z. Zhou, "Time domain integral equation solver using quadratic B-spline temporal basis

functions," *Microw. Opt. Techn. Lett.*, Vol. 49, 1154–1159, 2007.

15. Zhang, G. H. and M. Y. Xia, "Analysis of transient scattering by dielectric objects using time domain integral equation methods with parallel computing," *Acta Scientiarum Naturalium Uniersiatis Pekinensis*, Vol. 44, 353–356, 2008.
16. Sarkar, T. K., W. Lee, and S. M. Rao, "Analysis of transient scattering from composite arbitrarily shaped complex structures," *IEEE T. Antenn. Propag.*, Vol. 48, 1625–1634, 2000.
17. Rao, S. M. and T. K. Sarkar, "Numerical solution of time domain integral equation for arbitrarily shaped conductor/dielectric composite bodies," *IEEE T. Antenn. Propag.*, Vol. 50, 1831–1837, 2002.
18. Shanker, B., A. A. Ergin, and E. Michielssen, "Plane-wave-time-domain-enhanced marching-on-in-time scheme for analyzing scattering from homogeneous dielectric structures," *J. Opt. Soc. Am. A.*, Vol. 19, 716–726, 2002.
19. Shanker, B., A. A. Ergin, K. Aygün, and E. Michielssen, "Analysis of transient electromagnetic scattering from closed surfaces using a combined field integral equation," *IEEE T. Antenn. Propag.*, Vol. 48, 1064–1074, 2000.
20. Wang, P., M. Y. Xia, and L. Z. Zhou, "A study of accuracy of time domain integral equation methods for analysis of broadband electromagnetic scattering," *Acta Scientiarum Naturalium Uniersiatis Pekinensis*, Vol. 44, 62–66, 2008.
21. Jung, B. H., T. K. Sarkar, Y. S. Chung, et al., "Transient electromagnetic scattering from dielectric objects using the electric field integral equation with Laguerre polynomials as temporal basis functions," *IEEE T. Antenn. Propag.*, Vol. 52, 2329–2340, 2004.
22. Rao, S. M., D. R. Wilton, and A. W. Glisson, "Electromagnetic scattering by surfaces of arbitrary shape," *IEEE T. Antenn. Propag.*, Vol. 30, 409–418, 1982.